Mem. S.A.It. Vol. 78, 374

Memorie della

Dynamos in accretion discs

A. Brandenburg[1] and B. von Rekowski[2]

[1] NORDITA, AlbaNova University Center, SE-10691 Stockholm, Sweden;
e-mail: brandenb@nordita.dk
[2] School of Mathematics and Statistics, University of St. Andrews, North Haugh, St. Andrews, Fife KY16 9SS, UK

Abstract. It is argued that accretion discs in young stellar objects may have hot coronae that are heated by magnetic reconnection. This is a consequence of the magneto-rotational instability driving turbulence in the disc. Magnetic reconnection away from the midplane leads to heating of the corona which, in turn, contributes to driving disc winds.

Key words. ISM: jets and outflows — accretion, accretion discs — magnetohydrodynamics (MHD) — stars: mass-loss — stars: pre-main sequence

1. Introduction

Accretion discs provide the channel through which matter from the outside is able to collapse onto some common central object such as a protostar. Prior to the collapse, most of the matter will be in random motion and will have excess angular momentum with respect to the forming star. The disc allows the matter to get rid of this excess angular momentum, but in order to do this there needs to be some enhanced viscosity of some type. It is now generally accepted that this is provided by turbulence which is driven by the magneto-rotational instability (MRI; see Balbus & Hawley 1991, 1998).

An automatic by-product of MRI-driven turbulence is the possibility of significant resistive Joule heating in the layers away from the midplane, where the density is small and hence the heating per unit mass is large. This is demonstrated in Fig. 1, where we show that the total (magnetic and kinetic) stress, that leads to viscous and resistive heating, does not decrease with height away from the midplane, even though the product of rate of strain and density does decrease because of decreasing density. This was originally demonstrated only for nearly isothermal discs (Brandenburg et al. 1996a), see Fig. 1, but this has now also been shown for discs with full radiation transfer included (Turner 2004).

An important expectation from this is that the discs should be surrounded by hot coronae. In other words, not only the central protostar, but also the disc itself should be surrounded by hot coronae that are heated by the associated Joule (or resistive) heating via magnetic reconnection, as has been demonstrated in numerical experiments (Galsgaard & Nordlund 1996). This leads to the possibility of hot coronae with temperatures close to the Virial temperature, $T_{\rm vir}$, given by

$$c_p T_{\rm vir}(r) = GM_*/r, \quad (1)$$

Send offprint requests to: A. Brandenburg

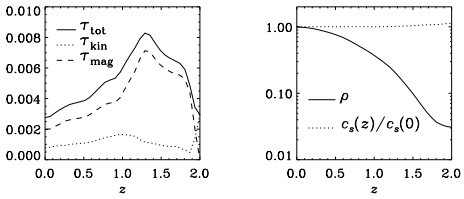

Fig. 1. Dependence of the stress component $\overline{\tau}_{\varpi\phi}$ (here denoted by $\tau_{\rm tot}$), separately for the kinetic and magnetic contributions, $\tau_{\rm kin}$ and $\tau_{\rm mag}$, respectively, together with the sum of the two denoted by total (left) as well as the vertical dependence of density and sound speed (right). Note that $\tau_{\rm tot}$ is neither proportional to the density ρ nor the sound speed $c_{\rm s}$. [Adapted from Brandenburg et al. (1996a).]

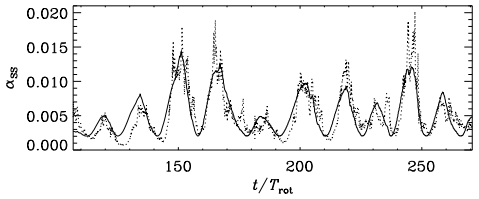

Fig. 2. Time series of the Shakura-Sunyaev viscosity alpha, $\alpha_{\rm SS}$. Here, time is normalized in terms of the orbital time, $T_{\rm rot} = 2\pi/\Omega$, where Ω is the local angular velocity. Note that $\alpha_{\rm SS}$ fluctuates strongly in time about an average value of around 0.01. [Adapted from Brandenburg (1998).]

where c_p is the specific heat at constant pressure, G is Newton's constant, M_* is the mass of the protostar, and r is the distance from the central object. The only process that can possibly counteract the tendency for strong coronal heating is radiative cooling. At present it is unclear what temperatures will be achieved if realistic cooling is included.

2. The mean accretion stress

The basic dynamics of the MRI can be modeled using simulations in a local cartesian geometry using shearing sheet boundary conditions in the radial direction. One of the main output parameters is the Shakura–Sunyaev viscosity parameter, $\alpha_{\rm SS}$, which is a nondimensional measure of the turbulent viscosity $\nu_{\rm t}$, in terms of the sound speed $c_{\rm s}$ and the disc scale height H, i.e.

$$\nu_{\rm t} = \alpha_{\rm SS} c_{\rm s} H. \tag{2}$$

Assuming that there is no external torque, this $\alpha_{\rm SS}$ is given by

$$\overline{\tau}_{\varpi\phi} = -\rho \nu_{\rm t} \varpi \frac{\partial \overline{\Omega}}{\partial \varpi}, \tag{3}$$

where ϖ is the cylindrical radius, ρ is the density, $\overline{\Omega}$ is the mean angular velocity, and $\overline{\tau}_{\varpi\phi}$ is the total 'horizontal' stress given by

$$\overline{\tau}_{\varpi\phi} = -\overline{b_\varpi b_\phi}/\mu_0 + \overline{\rho u_\varpi u_\phi}, \tag{4}$$

where $\boldsymbol{b}$ and $\boldsymbol{u}$ denote the fluctuating components of the magnetic and velocity fields, and μ_0 is the vacuum permeability. The first term, i.e. the magnetic stress, is usually the largest term. The resulting stress determined from the simulations and expressed in nondimensional form as $\alpha_{\rm SS}(t)$, is shown in Fig. 2. The simulation domain covers the upper disc plane only.

The expression in equation (3) would be used in the evolution equation for the mean angular velocity, $\overline{\Omega}$, where the term $\nu_{\rm t}$ would simply add to the microscopic viscosity ν to give a total viscosity, $\nu_{\rm T} = \nu_{\rm t} + \nu$. On the other hand, equation (4) would be used to determine $\overline{\tau}_{\varpi\phi}$, and hence $\alpha_{\rm SS}$, from three-dimensional simulation data.

The value of $\alpha_{\rm SS}(t)$ is notoriously small (around 0.01; see Hawley et al. 1996, Stone et al. 1996, Brandenburg et al. 1996b). Observational evidence suggests a typical range $\alpha_{\rm SS} \approx 0.1...0.4$ (King et al. 2007). Larger value of $\alpha_{\rm SS}$ can be obtained if there is an externally imposed magnetic field. Also global simulations tend to yield larger values (Hawley 2000).

The variation of $\alpha_{\rm SS}(t)$ shows a typical time scale of around 15 orbits. This is here a consequence of the emergence of cyclic large scale dynamo action. The magnetic field reverses between two maxima, so the actual period is actually around 30 orbits. Physically, this time is related to the turbulent diffusion time. This is now reasonably well understood and the details of the dynamo depend sensitively on the boundary conditions. Such cycles are not

expected in global geometry (Brandenburg & Campbell 1997).

3. The mean electromotive force

An important goal is to simulate outflows from discs that can produce a magnetic field. In other words, the magnetic field necessary for launching outflows is now no longer assumed as being given, but it is self-consistently generated in the disc, albeit in parameterized form. This feature was investigated by von Rekowski et al. (2003), who studied the possibility of collimated outflows in the *absence* of an ambient magnetic field. This idea seems now quite reasonable also from an observational point of view. Ménard & Duchêne (2004) report observations of the Taurus-Auriga molecular cloud which is a nearby star-forming region of low-mass stars. They find that jets and outflows from classical T Tauri star–disc systems in this cloud are not always aligned with the local magnetic field of the cloud where they are born. This suggests that jets are not likely to be driven by the cloud's own field. However, theoretical models have shown that magnetic fields are important for jet acceleration and collimation. Furthermore, there is now also observational evidence that jets and outflows are essentially hydromagnetic in nature. Observations of CO outflows exclude purely radiative and thermal driving of jets and outflows in regions of star formation of low-mass stars (Pudritz 2004). Thermal pressure might still be dynamically important to lift up the winds to the critical point. Moreover, there are observational indications of warm wind regions with temperatures of a few times 10^4 K (Gómez de Castro & Verdugo 2003). These winds cannot be due to stellar radiation because the star is too cool, suggesting that the warm winds are driven magnetohydrodynamically. So it is quite plausible that a disc dynamo might be necessary for the launching of jets and outflows.

In order to address problems such as the launching of disc winds from hot disc coronae, it is preferable to solve the equations in global geometry. This increases the computational demands, but some progress can be made by restricting oneself to axisymmetry. On the other hand, dynamo action is impossible in axisymmetry (Cowling 1933). However, it is sufficient to capture the essential three-dimensional effects in a statistical sense by considering the averaged equations.

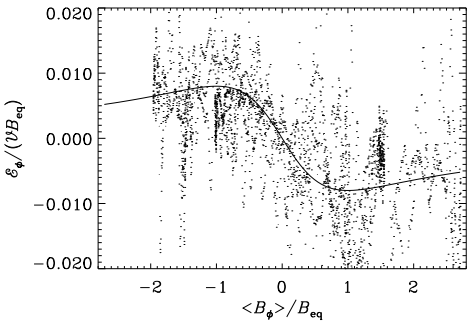

Fig. 3. Scatter plot of the volume averaged toroidal electromotive force, $\langle\mathcal{E}_\phi\rangle$, versus the volume averaged toroidal magnetic field strength $\langle B_\phi\rangle$. Here, $\langle\mathcal{E}_\phi\rangle$ is normalized with respect to the rms velocity $\mathcal{V}$ and the equipartition field strengths $B_{\rm eq} = \sqrt{\mu_0\rho\boldsymbol{u}^2}$. Both $\langle\mathcal{E}_\phi\rangle$ and $\langle B_\phi\rangle$ are obtained at different times during the simulation. Here μ_0 is the vacuum permeability. Note the negative slope in the diagram around $\langle B_\phi\rangle = 0$, indicating that the α effect in mean field dynamo theory is negative. The solid line represents a fit to a standard quenching law of the form $-\beta/(1+\beta^2)$, where $\beta = \langle B_\phi\rangle/B_{\rm eq}$. [Adapted from Brandenburg & Donner (1997).]

In the averaged equations the nonlinear terms lead to correlations, just like the stress terms considered in equation (4). In the present case there is the mean electromotive force,

$$\overline{\boldsymbol{\mathcal{E}}} = \overline{\boldsymbol{u}\times\boldsymbol{b}}, \tag{5}$$

where lower case $\boldsymbol{u}$ and $\boldsymbol{b}$ denote fluctuations, i.e. velocity and magnetic fields are split into mean and fluctuating components via $\boldsymbol{U} = \overline{\boldsymbol{U}} + \boldsymbol{u}$ and $\boldsymbol{B} = \overline{\boldsymbol{B}} + \boldsymbol{b}$. Equation (5) is used to determine $\overline{\boldsymbol{\mathcal{E}}}$ from simulation data. This expression is thus analogous to equation (4).

In isotropic turbulence $\overline{\boldsymbol{\mathcal{E}}} = 0$ (just like there is no off-diagonal terms in the stress considered above). However, in the presence of rotation and stratification $\overline{\boldsymbol{\mathcal{E}}}$ can be finite (Krause & Rädler 1980). In particular, theory suggests

that $\overline{\mathcal{E}}$ has a component along the direction of the mean field, i.e.

$$\overline{\mathcal{E}} = \alpha_{\rm dyn}\overline{\boldsymbol{B}} + ..., \quad (6)$$

where $\alpha_{\rm dyn}$ is the dynamo alpha which has the dimensions of a speed. The dots indicate the presence of additional terms such as turbulent resistivity, for example. The expression equation (6) would be used in a mean field model in the averaged induction equation for $\overline{\boldsymbol{B}}$, and is thus analogous to equation (3) which is used in the averaged momentum equation.

In Fig. 3 we show a scatter plot of the toroidal electromotive force, $\langle\mathcal{E}_\phi\rangle$, versus the volume averaged toroidal magnetic field strength $\langle B_\phi\rangle$ that has been obtained from a simulation of MRI-driven turbulence in the upper disc plane. Note the negative slope in the diagram indicating that the α effect in mean field dynamo theory is negative (Brandenburg et al. 1995, Ziegler & Rüdiger 2000). This is an unexpected result, because theory predicts $\alpha_{\rm dyn}$ to be positive in the upper disc plane. Various proposals for this negative sign have been put forward (Brandenburg 1998, Rüdiger & Pipin 2000, Blackman & Tan 2004). More detailed analysis confirms the negative value of $\alpha_{\rm dyn}$ and is also able to give its dependence on the distance from the midplane and other aspects (Brandenburg & Sokoloff 2002).

There is a great deal of work concerned with the possibility of so-called catastrophic quenching of $\alpha_{\rm dyn}$ that depends on the value of the microscopic magnetic Reynolds number. We cannot go into these aspects here, but we mention only that such quenching can be alleviated by magnetic helicity fluxes out of the domain (Blackman & Field 2000, Kleeorin et al. 2000), and that such fluxes can be driven by shear (Vishniac & Cho 2001, Subramanian & Brandenburg 2004, 2006). The end result might be an α effect that is no longer catastrophically quenched; see Brandenburg & Subramanian (2005) for a review. In the following we will just use this as an established fact, as has been done elsewhere in the literature (Campbell 2000, Bardou et al. 2001).

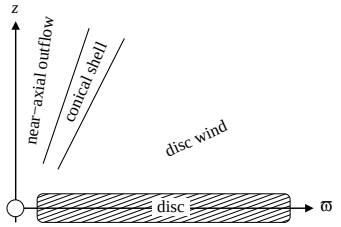

Fig. 4. General structure of the outflows typically obtained in the model of von Rekowski et al. (2003), where the cool, dense disc emits a thermally driven wind and a magneto-centrifugally driven outflow in a conical shell. [Adapted from von Rekowski et al. (2003).]

4. Structured outflows from discs

A mean field dynamo model with piece-wise polytropic hydrodynamics was proposed by von Rekowski et al. (2003). Like Ouyed & Pudritz (1997a,b) they start with an equilibrium corona, where they assume constant entropy and hydrostatic equilibrium according to $c_pT(r) = GM_*/r$. In order to make the disc cooler, a geometrical region for the disc is prescribed (see Fig. 4). An entropy contrast between disc and corona is chosen such that the initial disc temperature is about 3×10^3 K in the bulk of the disc. The low disc temperature corresponds to a high disc density of about $10^{-10} \ldots 10^{-9}$ g cm^{-3}. For the disc dynamo, the most important parameter is the dynamo coefficient $\alpha_{\rm dyn}$ in the mean field induction equation. The α effect is antisymmetric about the midplane and restricted to the disc.

The upper panel of Fig. 5 illustrates that an outflow develops that has a well-pronounced structure. Within a conical shell originating from the inner edge of the disc, the terminal outflow speed exceeds 500 km/s, and temperature and density are lower than elsewhere. The inner cone around the axis is the hottest and densest region where the stellar wind speed reaches about 150 km/s. The wind that develops from the outer parts of the disc has intermediate values of the speed.

The structured outflow is driven by a combination of different processes. A significant amount of angular momentum is transported outwards from the disc into the wind along

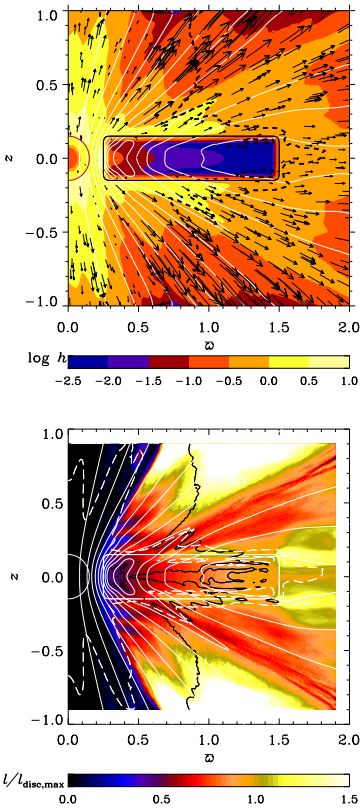

Fig. 5. Upper panel: poloidal velocity vectors and poloidal magnetic field lines (white) superimposed on a color scale representation of $\log h$. Specific enthalpy h is directly proportional to temperature T, and $\log h = (-2,-1,0,1)$ corresponds to $T \approx (3{\times}10^3, 3{\times}10^4, 3{\times}10^5, 3{\times}10^6)$ K. The black dashed line shows the fast magnetosonic surface. The disc boundary is shown with a thin black line, the stellar surface is marked in red. The dynamo $\alpha_{\rm dyn}$ coefficient is negative in the upper disc half, resulting in roughly dipolar magnetic symmetry. Averaged over times $t \approx 897 \ldots 906$ days. Lower panel: color scale representation of the specific angular momentum, normalized by the maximum angular momentum in the disc, with poloidal magnetic field lines superimposed (white). The black solid line shows the Alfvén surface, the white dashed line the sonic surface. Same model as in the upper panel and averaged over same times. [Adapted from von Rekowski & Brandenburg (2004).]

the magnetic field, especially along the strong lines within the conical shell (see the lower panel of Fig. 5). The magnetic field geometry is such that the angle between the rotation axis and the field lines threading the disc exceeds 30° at the disc surface, which is favorable for magneto-centrifugal acceleration (Blandford & Payne 1982). However, the Alfvén surface is so close to the disc surface at the outer parts of the disc that acceleration there is mainly due to the gas-pressure gradient. In the conical shell, however, the outflow is highly supersonic and yet sub-Alfvénic, with the Alfvén radius a few times larger than the radius at the footpoint of the field lines at the disc surface. The lever arm of about 3 is sufficient for magneto-centrifugal acceleration to dominate in the conical shell (cf. Krasnopolsky et al. 1999).

5. Star–disc coupling

The interaction of a stellar magnetic field with a circumstellar accretion disc and its magnetic field was originally studied in connection with accretion discs around neutron stars (Ghosh & Lamb 1979), but it was later also applied to protostellar magnetospheres (Königl 1991, Cameron & Campbell 1993, Shu et al. 1994). Most of the work is based on the assumption that the field in the disc is constantly being dragged into the inner parts of the disc from large radii. The idea behind this is that a magnetized molecular cloud collapses, in which case the field in the central star and that in the disc are aligned (Shu et al. 1994). This was studied numerically by Hirose et al. (1997) and Miller & Stone (1997). In the configurations they considered, there is an X-point in the equatorial plane (see left hand panel of Fig. 6), which can lead to a strong funnel flow.

The other alternative has been explored by Lovelace et al. (1995) where the magnetic field of the star has been flipped and is now antiparallel with the field in the disc, so that the field in the equatorial plane points in the same direction and has no X-point. However, current sheets develop above and below the disc plane (see right hand panel of Fig. 6). This configuration is also referred to as the X-wind model. Ironically, this is the field configuration without an X-point.

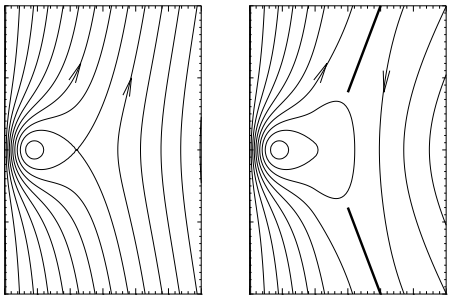

Fig. 6. Sketch showing the formation of an X-point when the disc field is aligned with the dipole (on the left) and the formation of current sheets with no X-point if they are anti-aligned (on the right). The two current sheets are shown as thick lines. In the present paper, the second of the two configurations emerges in all our models, i.e. with current sheets and no X-point. [Adapted from von Rekowski & Brandenburg (2004).]

Numerical simulations of such a field configuration by Hayashi et al. (1996) confirm the idea by Lovelace et al. (1995) that closed magnetic loops connecting the star and the disc are twisted by differential rotation between the star and the disc, and then inflate to form open stellar and disc field lines (see also Bardou 1999, Agapitou & Papaloizou 2000, Uzdensky et al. 2002). Goodson et al. (1997,1999) and Goodson & Winglee (1999) find that for sufficiently low resistivity, an accretion process develops that is unsteady and proceeds in an oscillatory fashion. The same result has also been obtained by von Rekowski & Brandenburg (2004). It should be emphasized that in their case the resulting field geometry is always the second one in Fig. 6, i.e. the one with current sheets and no X-point. The inflating magnetosphere expands to larger radii where matter can be loaded onto the field lines and be ejected as stellar and disc winds. Reconnection of magnetic field lines allows matter to flow along them and accrete onto the protostar, in the form of a funnel flow (see also Romanova et al. 2002). Consequently, the outflows show episodic behavior; see also Matt et al. (2002) and von Rekowski & Brandenburg (2004).

In the model of von Rekowski & Brandenburg (2004) the highly episodic accretion flow and accretion rate are correlated with the configuration of the magnetosphere. Low values of B_z at the position $(\varpi, z) = (0.6, 0.4)$, correspond to a configuration were closed magnetospheric lines penetrate the inner disc edge, thus connecting the star to the disc (as in the left hand panel of Fig. 7). In this case, disc matter is loaded onto magnetospheric field lines and flows along them to accrete onto the star. As a consequence, the accretion rate is highest during these phases, typically up to between $10^{-8} M_\odot\,\mathrm{yr}^{-1}$ and $2.5 \times 10^{-8} M_\odot\,\mathrm{yr}^{-1}$.

High values of B_z at the position $(\varpi, z) = (0.6, 0.4)$, correspond to a configuration when the outer field lines of the magnetosphere have opened up into disconnected open stellar and disc field lines, thus disconnecting the star from the disc (as in the right hand panel of Fig. 7). In this case, matter is lost directly into the outflow and there is no net accretion of disc matter.

6. Conclusions

Simulations of disc dynamos as well as of star-disc coupling have shown several surprises that were not originally expected. On the other hand, some of these results are still only tentative and one cannot really be sure to what extent they are artifacts of the model setup or other technical limitations. The fact that $\alpha_{\rm dyn}$ is negative in the upper disc plane is one such result that has so far only been obtained in the local shearing box simulations. It would be good to check this result independently using global models. Most of the recent global simulations tend to focus on the magnetic field structures and their effects on the gas rather than on studying the magnetic field *generation*, for example by identifying parameterizations that could be used for mean field modeling.

Regarding star–disc coupling there are questions concerning the strength of numerical viscosity and other technical aspects that make it difficult to be sure about the significance of the result. Here, however, the basic processes involved are now well understood, in particular the inflation of field lines that are being differentially sheared are they permeate the disc. As argued by Matt & Pudritz

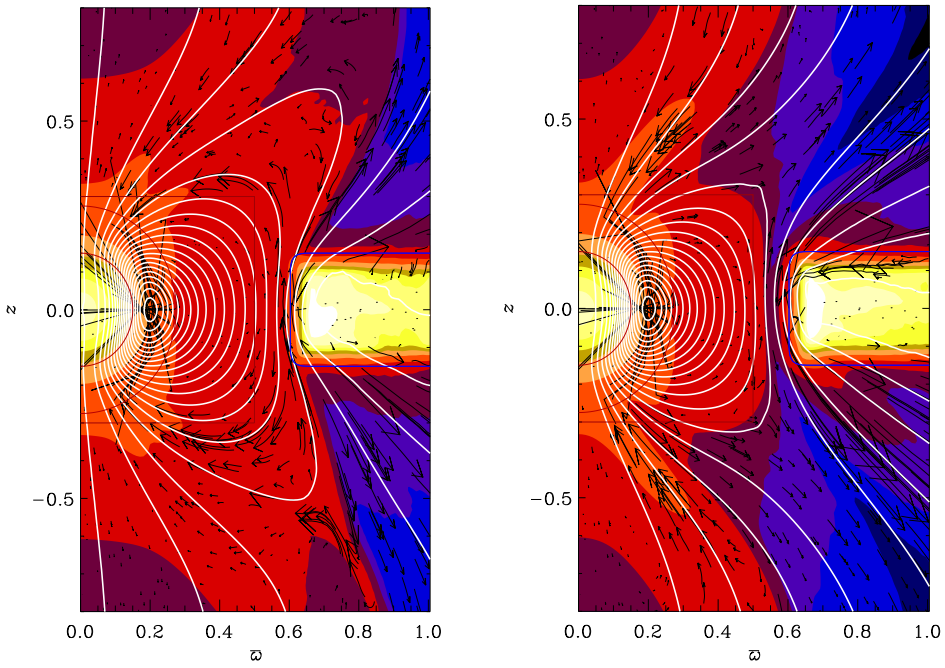

Fig. 7. Colour/grey scale representation of the density (bright colors or light shades indicate high values; dark colors or dark shades indicate low values) with poloidal magnetic field lines superimposed (white) and the azimuthally integrated mass flux density, represented as the vector $2\pi\varpi\varrho(u_\varpi, u_z)$, shown with arrows (except in the disc where the density is high and the mass flux vectors would be too long). The left hand panel is at the time $t = 98$ when the star is magnetically connected to the disc and the right hand panel is at the time $t = 102$ when the star is magnetically disconnected from the disc. [Adapted from von Rekowski & Brandenburg (2004).]

(2004, 2005), this makes the disc-locking of the star rather inefficient. This motivates the search for other mechanisms facilitating stellar braking. A plausible candidate is braking by a stellar wind, which was also found by von Rekowski & Brandenburg (2006). Extending these types of calculations to three dimensions and to higher resolution remain important future tasks (see, e.g., von Rekowski & Piskunov 2006 for initial studies).

Acknowledgements. Use of the supercomputer SGI 3800 in Linköping and of the PPARC supported supercomputers in St Andrews and Leicester is acknowledged. This research was conducted using the resources of High Performance Computing Center North (HPC2N). The Danish Center for Scientific Computing is acknowledged for granting time on the Linux cluster in Odense (Horseshoe).

References

Agapitou, V., & Papaloizou, J. C. B. 2000, MNRAS, 317, 273
Balbus, S. A., & Hawley, J. F. 1991, ApJ, 376, 214
Balbus, S. A. & Hawley, J. F. 1998, Rev. Mod. Phys., 70, 1
Bardou, A. 1999, MNRAS, 306, 669
Bardou, A., Rekowski, B. v., Dobler, W., et al. 2001, A&A, 370, 635
Blackman, E. G., & Tan, J. C. 2004, Ap&SS, 292, 395
Blackman, E. G., & Field, G. B. 2000, MNRAS, 318, 724
Blandford, R. D., & Payne, D. R. 1982, MNRAS, 199, 883

Brandenburg, A. 1998, in Theory of Black Hole Accretion Discs, ed. M. A. Abramowicz, G. Björnsson & J. E. Pringle (Cambridge University Press), 61
Brandenburg, A., & Campbell, C. G. 1997, in Accretion disks – New aspects, ed. H. Spruit & E. Meyer-Hofmeister (Springer), 109
Brandenburg, A., & Donner, K. J. 1997, MNRAS, 288, L29
Brandenburg, A., & Sokoloff, D. 2002, Geophys. Astrophys. Fluid Dyn., 96, 319
Brandenburg, A., & Subramanian, K. 2005, Phys. Rep., 417, 1
Brandenburg, A., et al. 1995, ApJ, 446, 741
Brandenburg, A., et al. 1996a, in Physics of Accretion Disks, ed. S. Kato, S. Inagaki, S. Mineshige & J. Fukue (Gordon and Breach), 285
Brandenburg, A., Nordlund, Å, Stein, R. F., et al. 1996b, ApJ, 458, L45
Cameron, A. C., & Campbell, C. G. 1993, A&A, 274, 309
Campbell, C. G. 2000, MNRAS, 317, 501
Cowling, T. G. 1933, MNRAS, 94, 39
Galsgaard, K., & Nordlund, Å. 1996, J. Geophys. Res., 101, 13445
Gómez de Castro, A. I., & Verdugo, E. 2003, ApJ, 597, 443
Goodson, A. P., & Winglee, R. M. 1999, ApJ, 524, 159
Goodson, A. P., Böhm, K.-H., & Winglee, R. M. 1999, ApJ, 524, 142
Goodson, A. P., Winglee, R. M., & Böhm, K.-H. 1997, ApJ, 489, 199
Ghosh, P., & Lamb, F. K. 1979, ApJ, 232, 259
Hawley, J. F. 2000, ApJ, 528, 462
Hawley, J. F., Gammie, C. F., & Balbus, S. A. 1996, ApJ, 464, 690
Hayashi, M. R., Shibata, K., & Matsumoto, R. 1996, ApJ, 468, L37
Hirose, S., et al. 1997, Publ. Astron. Soc. Japan, 49, 193
King, A. R., Pringle, J. E., & Livio, M. 2007, arXiv:astro-ph/0701803
Kleeorin, N., Moss, D., Rogachevskii, I., & Sokoloff, D. 2000, A&A, 361, L5
Königl, A. 1991, ApJ, 370, L39
Krasnopolsky, R., Li Z.-Y., and Blandford R. D. 1999, ApJ, 526, 631
Krause, F., & Rädler, K.-H. 1980, Mean-Field Magnetohydrodynamics and Dynamo Theory (Pergamon Press, Oxford)
Lovelace, R. V. E., Romanova, M. M., & Bisnovatyi-Kogan, G. S. 1995, ApJ, 275, 244
Matt, S., & Pudritz, R. E. 2004, ApJ, 607, L43
Matt, S., & Pudritz, R. E. 2005, MNRAS, 356, 167
Matt, S., et al. 2002, ApJ, 574, 232
Ménard, F., & Duchêne, G. 2004, A&A, 425, 973
Miller, K. A., & Stone, J. M. 1997, ApJ, 489, 890
Ouyed, R., & Pudritz, R. E. 1997a, ApJ, 482, 712
Ouyed, R., & Pudritz, R. E. 1997b, ApJ, 484, 794
Pudritz, R. E. 2004, Ap&SS, 292, 471
Romanova, M. M., Ustyugova, G. V., Koldoba, A. V., et al. 2004, ApJ, 616, L151
Rüdiger, G., & Pipin, V. V. 2000, A&A, 362, 756
Shu, F., Najita, J., Ostriker, E., et al. 1994, ApJ, 429, 781
Stone, J. M., Hawley, J. F., Gammie, C. F., et al. 1996, ApJ, 463, 656
Subramanian, K., & Brandenburg, A. 2004, Phys. Rev. Lett., 93, 205001
Subramanian, K., & Brandenburg, A. 2006, ApJ, 648, L71
Turner, N. J. 2004, ApJ, 605, L45
Uzdensky, D. A., Königl, A., & Litwin, C. 2002, ApJ, 565, 1191
Vishniac, E. T., & Cho, J. 2001, ApJ, 550, 752
von Rekowski, B., & Brandenburg, A. 2004, A&A, 420, 17
von Rekowski, B., & Brandenburg, A. 2006, Astron. Nachr., 327, 53
von Rekowski, B., & Piskunov, N. 2006, Astron. Nachr., 327, 340
von Rekowski, B., Brandenburg, A., Dobler, W., et al. 2003, A&A, 398, 825
Ziegler, U., & Rüdiger, G. 2000, A&A, 356, 1141